HHS Public Access

Author manuscript

Nature. Author manuscript; available in PMC 2013 November 30.

Published in final edited form as:

Nature. 2013 May 30; 497(7451): 624–627. doi:10.1038/nature12146.

mSWI/SNF (BAF) Complexes Facilitate Decatentation of DNA by Topoisomerase IIα

Emily C. Dykhuizen[*,1,2], **Diana C. Hargreaves**[*,1,2], **Erik Miller**[1,2], **Kairong Cui**[7], **Andrey Korshunov**[3], **Marcel Kool**[4], **Stefan Pfister**[4,5], **Yoon-Jae Cho**[6], **Keji Zhao**[7], and **Gerald R. Crabtree**[1,2]

[1]Department of Pathology Stanford University School of Medicine, Stanford CA 94305

[2]Howard Hughes Medical Institute, Stanford University School of Medicine, Stanford CA 94305

[3]CCU Neuropathology, German Cancer Research Center (DKFZ), Im Neuenheimer Feld 280, Heidelberg 69120, Germany

[4]Division of Pediatric Neurooncology, German Cancer Research Center (DKFZ), Im Neuenheimer Feld 280, Heidelberg 69120, Germany

[5]Department of Pediatric Oncology, University Hospital Heidelberg, Im Neuenheimer Feld 430, Heidelberg 69120, Germany

[6]Department of Neurology and Neurosurgery, Stanford University Medical School, Stanford, CA 94305

[7]National Institutes of Health, Bethesda, MD

Abstract

Recent exon sequencing studies of human tumors have revealed that subunits of mSWI/SNF or BAF complexes are mutated in more than 20% of all human malignancies,[1,2] yet the mechanisms involved in tumor suppression are unclear. BAF chromatin remodeling complexes are polymorphic assemblies that use energy provided by ATP hydrolysis to regulate transcription through the control of chromatin structure[3] and the placement of Polycomb (PcG) across the genome[4,5]. Several proteins dedicated to this multi-subunit complex, including SMARCA4 (BRG1) and BAF250A (ARID1A), are mutated at frequencies similar to that of recognized tumor suppressors. In particular, the core ATPase BRG1 is mutated in 5-10% of childhood medulloblastoma[6-9] and greater than 15% of Burkitt's Lymphoma.[10,11] Here we find a novel function of BAF complexes in decatenating newly replicated sister chromatids, a requirement for

Correspondence and requests for materials should be addressed to G.R.C. (crabtree@stanford.edu).

*These authors contributed equally to this work.

Supplementary Information accompanies this paper

Author Contribution Statement and Accession Numbers: E.C.D., D.C.H., and G.R.C. designed the experiments, and E.C.D. and D.C.H. performed the experiments. E.M. performed bioinformatic analysis. A.K., M.K., S.P., and Y-J.C. contributed human tumor samples. K.Z. and K.C. performed sequencing of the TopoIIα ChIP. E.C.D., D.C.H, and G.R.C. wrote the manuscript. The accession number for the TopoIIα ChIP-Seq is GSE45625

The authors declare no competing interests

proper chromosome segregation during mitosis. We find that deletion of Brg1, as well as the expression of Brg1 point mutants identified in human tumors leads to anaphase bridge formation (sister chromatids linked by catenated strands of DNA), and a G_2/M phase block characteristic of the decatenation checkpoint. Endogenous BAF complexes directly interact with endogenous TopoIIα through BAF250a and are required for TopoIIα binding to about 12,000 sites over the genome. Our results demonstrate that TopoIIα's chromatin binding is dependent on the ATPase activity of Brg1, which is compromised in oncogenic Brg1 mutants. These studies indicate that the ability of TopoIIα to prevent DNA entanglement at mitosis requires BAF complexes and suggest that this activity contributes to the role of BAF subunits as tumor suppressors.

Using Brg1$^{flox/flox}$;actin-CreER embryonic stem (ES) cells (Brgf/f), we observed that tamoxifen-induced deletion of Brg1 (Brgf/fERΔ) results in the appearance of DNA bridges during anaphase (Fig. 1a). This phenotype is characteristic of a deficiency in TopoIIα function, which normally resolves DNA catenanes that develop during transcription and replication[12]. We determined the frequency of anaphase bridges in Brgf/fERΔ cells to be similar to that of cells deficient in other putative tumor suppressors that regulate TopoIIα function, including BRCA1, RanBP2, and RECQL5[13-15] (Fig. 1a).

In previous studies, we recovered peptides from TopoIIα in mass spectrometric analysis of endogenous BAF complexes[16]. Immunoprecipitation (IP) of BAF complexes with antibodies to Brg1 recovered TopoIIα and, conversely, IP of TopoIIα revealed Brg1 (Fig. 1b). This association is not dependent on DNA (Supplementary Fig.1a, b). We detected this association in several additional cell types, including mouse embryonic fibroblasts (MEFs) and HEK293Ts (Supplementary Fig. 1c).

Failure of TopoIIα to resolve catenated DNA leads to slow progression through the G_2/M phase of the cell cycle[17]. To better understand the mitotic defect in Brg1-deficient cells, we synchronized Brgf/f and Brgf/fERΔ cells in G_1/S using double-thymidine block. Following release, Brgf/f and Brgf/fERΔ cells transited through the cell cycle at the same rate until reaching G_2/M, where the Brgf/fERΔ cells exhibited a significant delay (Fig. 1c). In asynchronously dividing cells, this delay resulted in a 1.5- to 2-fold increase in Brgf/fERΔ cells in G_2/M (Fig. 1d), similar to the treatment of cells with the TopoII inhibitor ICRF-193[18]. Caffeine, an inhibitor of ATM/ATR, forces cells through an ICRF-193-induced decatenation checkpoint[18] and similarly overrides the G_2/M arrest in Brgf/fERΔ cells (Fig. 1d). Furthermore, expression of TopoIIαS1524A, which fails to recruit MDC1 to chromatin upon initiation of the decatenation checkpoint[19], alleviated the cell cycle delay, suggesting that Brgf/fERΔ cells arrest due to activation of the decatenation checkpoint (Fig. 1e, supplementary Fig. 1d). Finally, chromosomes from Brgf/fERΔ cells are significantly longer than chromosomes from Brgf/f cells (Fig. 1f, supplementary Fig. 1e),a defect observed in TopoIIα-deficient cells due to its role in chromosome condensation[12,20]. These data indicate that Brg1 deletion resembles the mitotic defects observed with chemical inhibition and/or knockdown of TopoIIα[12,17,18,20].

We investigated oncogenic point mutants of Brg1 found in medulloblastoma and Burkitt's lymphoma (Brg1G1232D (BrgGD) and Brg1T910M (BrgTM)[6-11]) by expressing FLAG-tagged versions in Brgf/f cells (Fig. 2a). The Brg1 mutants were incorporated into the BAF

complex normally and did not alter the composition of the complex (supplementary Fig 2a). Although T910M is located in the ATP binding pocket of Brg1, the G1232D mutation is downstream of HELICc domain and thus not obviously involved in ATP turnover (Fig. 2a). Subjecting BAF complexes containing BrgGD, BrgTM, BrgWT, or Brg1K798R (BrgKR)[21], the ATPase-dead point mutant of Brg1, to an assay for ATPase activity revealed that both cancer mutants are significantly compromised in ATPase activity, though not as profoundly as BrgKR (Fig. 2b). BrgTM is more severely compromised than BrgGD, which correlated with the viability of the respective cell line (supplementary Fig 2b).

Cells expressing BrgGD and BrgTM, but not BrgWT, display increases in the percentage of G_2/M cells and the incidence of anaphase bridges similar to that of Brgf/fERΔ cells (Fig. 2c, d). Importantly, expression of the mutants in the presence of endogenous Brg1 gives similar increases, although less severe, in G_2/M percentage and anaphase bridge incidence compared to vector cells (Fig. 2c, d). The dominant nature of these mutants on cell cycle and anaphase bridge formation suggests that medulloblastomas with both heterozygous and homozygous mutations in Brg1 have these mitotic defects.

To explore whether the increase in anaphase bridges contributes to increased chromosome instability as it does in TopoIIα-deficient cells[12,17], we analyzed ploidy in the Brg1 mutant cell lines. Expression of BrgGD or BrgTM results in a significant increase in cells with >4N DNA content in both ethanol- and tamoxifen-treated cells (Fig. 2c, supplementary Fig 2c). We also observed a significant increase in the number of BrgGD and BrgTM expressing cells with abnormal chromosome number in metaphase spreads from both ethanol- and tamoxifen-treated samples (Fig. 2e). These data suggest that G1232D and T910M mutations in Brg1 can contribute to chromosome instability as a result of deficiencies in TopoIIα function.

We collected several BRG1 mutant medulloblastomas to determine whether the effects of TopoIIα deficiency can be observed in primary tumors. We observed an increased proportion of anaphase bridges in each of five histologic samples from BRG1 mutant tumors relative to controls, suggesting these tumors have decatenation defects (Fig. 2f, supplementary Fig 2d). Aneuploidy is common in medulloblastoma and ranges from the partial gain or loss of single chromosomes to full tetraploidy[8,22,23]. However, a recent study showed that the relative rate of tetraploidy of 5 BRG1 mutant tumors was similar to that of 15 BRG1 WT tumors[8]. Additional sample characterization will be necessary to definitively assess whether BRG1 mutation causes mitotic defects through insufficient TopoIIα function in medulloblastoma.

Microarray analysis of Brgf/f and Brgf/fERΔ ES cells indicated that Brg1-dependent genes are not enriched for GO terms related to DNA damage or repair[24]. Additionally, we found no alterations in the abundance, post-translational modifications, cellular localization, or *in vitro* enzymatic activity of TopoIIα in Brgf/fERΔ cells (supplementary Fig. 3a-f, Supplementary 4). To test whether purified BAF complexes could enhance the enzymatic activity of recombinant TopoIIα, we used the standard *in vitro* kinetoplast DNA-based decatenation assay. Immobilized BAF complexes increased TopoIIα's enzymatic activity (Supplementary Fig 5a); however, Brg1 mutant BAF complexes also enhanced TopoIIα's

activity, as did PRC2, indicating a nonspecific activity on a bare DNA template[25] that does not reflect our *in vivo* observations. The Brg1 mutants did however reduce TopoIIα's association with chromatin, such that more TopoIIα remained associated with chromatin after high salt wash in BrgWT cells than in BrgTM, BrgGD, and vector cells (Fig. 3a, Supplementary Fig 5b, c). Reduced binding of TopoIIα to chromatin would be expected to compromise TopoIIα function and could represent an inability of TopoIIα to associate with substrate DNA during decatenation.

To identify defined regions of TopoIIα binding across the genome, we performed a TopoIIα ChIP-seq in Brgf/f and Brgf/fERΔ cells. We recovered very few peaks using traditional ChIP methods, so we employed etoposide, a small molecule that freezes TopoIIα in a covalent complex with DNA during the enzymatic process, thereby identifying sites of active TopoIIα cleavage[26]. We recovered 16591 TopoIIα peaks in Brgf/f cells and 4623 TopoIIα peaks in Brgf/fERΔ cells, demonstrating the contribution of Brg1 to TopoIIα binding (Fig. 3b). Almost two thirds of the TopoIIα Brgf/f peaks are DNase I hypersensitive, consistent with TopoIIα's preference for nucleosome-free DNA[27]. An example reflecting these trends is shown in Figure 3c. We confirmed TopoIIα binding by ChIP-qPCR at 14 Brg1-dependent and 10 Brg1-independent sites in Brgf/f and Brgf/fERΔ cells (Fig. 3d). Additionally, we determined that TopoIIα binding is mitigated in BrgTM and BrgGD mutant Brgf/fERΔ cells at Brg1-dependent sites (Fig. 3e). This is not the result of reduced binding of the Brg1 mutants to chromatin, as BrgTM and BrgGD bind similarly to BrgWT at these sites (Fig. 3f). Given that the BrgTM and BrgGD mutants display reduced ATPase activity, these data implicate a role for the ATP-dependent accessibility activity of BAF complexes in TopoIIα binding and function across the genome, a function previously identified for yeast Snf5 in transcription[28].

Due to the dedicated nature of subunits within BAF complexes, TopoIIα could be interacting with any BAF subunit. Indeed, we precipitated TopoIIα with antibodies to several dedicated subunits as determined by glycerol gradient centrifugation analysis (Fig. 4a, Supplementary Fig 6a). Quantitation of the precipitated TopoIIα revealed that little TopoIIα was recovered after IP with antibodies raised against BAF250a (aa1236-1325) and BAF250b (aa1300-1350), while other antibodies immunoprecipitated TopoIIα well (Fig 4a). We reasoned that the BAF250a/b antibody might disrupt the interaction between TopoIIα and the BAF complex if TopoIIα bound directly to BAF250a/b. Indeed, TopoIIα associated with full-length BAF250a and BAF250a (aa1-1758), but not BAF250a (aa1759-2285) in a heterologous expression system (Fig. 4b). This interaction is independent of Brg1 because we were unable to detect Brg1 in co-precipitates of BAF250a (aa1-1758) and TopoIIα. Furthermore, the association between TopoIIα and Brg1 was lost upon knockdown of BAF250a, with the most severe knockdown resulting in the most severe loss of association (Fig. 4c, Supplementary Fig 6b). To determine whether the interaction between TopoIIα and BAF250a was physiologically relevant, we knocked down BAF250a in MEFs and observed frequencies of anaphase bridges and G_2/M delay similar to knockdown of Brg1 or TopoIIα (Fig. 4d, e, Supplementary Fig. 6c, d). These data indicate that TopoIIα associates with Brg1 via a direct interaction with BAF250a.

Our studies point to a new role for ATP-dependent chromatin remodeling in decatenating DNA. Reduced decatenation *in vivo* is revealed by the frequency of anaphase bridges and an increase in the number of cells in G_2/M upon deletion of Brg1 or expression of the tumor-associated T910M and G1232D Brg1 mutants (Fig. 1a, d, Fig. 2c, d). Although mitotic defects have been noted in cells lacking Brg1, the cause of these defects was unclear[29]. In addition to Brg1, loss of BAF250a also results in decatenation defects (Fig. 4d, e), which could reflect the high incidence of mutations in BRG1 and BAF250A (ARID1A) in human tumors[1,23]. Our *in vivo* observations are reinforced by the requirement of BAF for TopoIIα binding at DNase I hypersensitive Brg1-binding sites (Fig. 3b-e).

The dependence of TopoIIα on BAF function offers a possible explanation for the frequency with which BAF subunit mutations are detected in screens for driving mutations in human cancers. Anaphase bridges are often forcibly severed during cytokinesis[30], resulting in partial or complete chromosome gains or losses as well as polyploidy if the cell fails to undergo mitosis[12,17]. At present, the number of BRG1 mutant medulloblastomas analyzed for ploidy status is insufficient to determine whether BRG1 mutation results in aneuploidy in human tumors. In the case of medulloblastoma, mutations in Brg1 are often accompanied by activating mutations in the WNT signaling pathways and/or MYC amplification[23]. Further studies highlighting these pairings will help define the contribution of reduced TopoIIα function as a result of BRG1 mutation to tumorigenesis.

Methods

Brg1 deletion from Brgf/fCreER ES cells and MEFs was performed as previously described[4]. Lentiviruses were produced in HEK293T cells using PEI transfection. Cells were synchronized using double thymidine block. Cell cycle analysis was performed according to manufacturer instructions (BD Biosciences). TopoIIα ChIP-seq was performed following etoposide fixation[26]. Real-time PCR, immunofluorescence, immunoprecipitation, and western blotting were done using standard protocols. The chromatin fraction from nuclei in varying concentrations of NaCl was analyzed by western blot.

Immunofluorescence

To quantitate anaphase bridges, cells were fixed with 4% paraformaldehyde for 20 minutes, washed, and stained with DAPI (Sigma). The number of anaphases/telophases with bridges over the total number of anaphases (between 56-187 total anaphases per 25mm slide) was recorded from each slide for more than four independent experiments. Brgf/f and Brgf/fERΔ ES cells were visualized with DAPI 72 hours after tamoxifen treatment. WT MEFs infected with lentiviruses containing hairpins to Brg1, BAF250a or TopoIIα and analyzed 48-96 hours after infection.

To stain for TopoIIα and centromeres/microtubules, cells were blocked with 5% BSA/1% goat serum in PBST for 1 hour following fixation and incubated with anticentromere (Antibodies Inc 15-235) or anti-γtubulin (Sigma T5326) and anti-TopoIIα (Santa Cruz sc-365916) for 2 hours. Following several washes, anti-human AlexFluor488 and anti-rabbit AlexaFluor568 were added for 1 hour. The cells were then stained with DAPI for 10

minutes and washed 3×PBS for 10 minutes each. The coverslips were mounted on slides with Vectashield Hardmount (Vector Labs, Burlingame, CA).

To quantitate anaphase bridges from paraffin-embedded human tumor samples, slides were incubated 2×25 minutes in xylenes, then rehydrated in 100% EtOH, then 95% EtOH, then water for 2 minutes each. The slides were boiled in Citrate Buffer (pH 6.0) (Vector Labs, Burlingame, CA) for 20 minutes and washed 2×5 minutes in PBS-Tween. The slides were then stained with DAPI for 10 minutes and washed 3×5 minutes with PBS before mounting with Vectashield Hardmount.

Cell synchronization

ES cells were incubated with 2mM thymidine for 7-8 hours, released into fresh media for 7 hours, and then incubated with thymidine again for 7 hours. The cells were washed several times with PBS, released into fresh media, and harvested at time points thereafter.

Cell Cycle analysis

The cell cycle analysis was performed using BD Biosciences BrdU-FITC FACS kit. ES cells were incubated with BrdU for 1 hour and MEFs were incubated with BrdU for 4 hours. Brgf/f and Brgf/fERΔ ES cells were analyzed 72 hours after tamoxifen treatment. Caffeine was added to media 2 hours before BrdU incubation. To determine the percent of cells in G2/M, DNA was stained with 7AAD and analyzed by FACS.

H3(S10)P cell cycle analysis

Brgf/f ES cells were infected with RNAi-resistant wild-type hTopoIIα or hTopoIIαS1524A and shRNAs to mouse TopoIIα. Cells were stained with anti-H3(S10)P and analyzed by flow cytometry 72 hours after treatment with or without tamoxifen.

Metaphase Spread Preparation

MEFs were grown to 85% confluence and incubated for 4 hours with colcemid. Cells were harvested and swelled by dropwise addition of 1:1 0.4% KCl/0.4% Sodium Citrate for 7 minutes at 37°C. Cells were then fixed by dropwise addition of 3:1 MeOH/Acetic Acid for 20 minutes, spun down, and fixed for another 30 minutes. Metaphases were dropped onto slides, dried on wet paper towels and stained with DAPI for visualization. Chromosomes were then measured and counted using ImageJ software. To analyze polyloidy, only cells with greater than 35 chromosomes were counted to eliminate artifacts due to partial spreads.

Gene Expression Profiling and Analysis

RNA was isolated using TRIzol (Invitrogen) and reverse transcribed into cDNA using SuperScript III reverse transcriptase (Invitrogen). Real-time PCR was performed on the StepOnePlus (ABI) machine using FastStart Universal SYBR Green Master with ROX (Roche).

Immunoprecipitation

Nuclei were isolated from cells with Buffer A (25 mM Hepes, pH7.6, 5 mM $MgCl_2$, 25 mM KCl, 0.05 mM EDTA, 10% glycerol, 0.1% NP-40) and lysed for 30 min in IP buffer (50 mM Tris-HCl, pH 8.0, 150 mM NaCl, 0.1% NP-40). The chromatin was removed using centrifugation and the lysates were precleared with 20 μL protein A or protein G dynabeads for 30 min. The protein concentration was quantitated using the BCA assay and adjusted to a final volume of 200 μL at a final concentration of 1.5 mg/mL with IP buffer. Each IP was incubated with 3 μg of anti-Brg1 (Santa Cruz sc-17796), anti-TopoIIα (Abcam ab52934), anti-BAF45d (Crabtree Lab), anti-BAF47 (Santa Cruz sc-166165), anti-BAF57 (Bethyl A300-810A), anti-BAF155 (Crabtree Lab), anti-BAF60a (BD Transduction Laboratories 611728), anti-BAF250a (Santa Cruz sc-32761x, Santa Cruz sc-98441X), anti-BAF180 (Bethyl A301-590A), anti-BAF250b (Santa Cruz sc-32762X, Bethyl A301-046A), anti-SS18 (Santa Cruz sc-28698) BAF200 (Santa Cruz sc-98299X) or anti-IgG (Santa Cruz sc-2025) overnight at 4°C and then for 2h with 20 μL protein A/G dynabeads. The beads were washed four times with 1 mL IP buffer and resuspended in 10 μL gel loading buffer (4× LDS Buffer; Invitrogen).

Glycerol Gradient Centrifugation Analysis

ES cells were lysed in Buffer A (10 mM Hepes (pH 7.6), 25 mM KCl, 1 mM EDTA, 10% glycerol, 1 mM DTT, and protease inhibitors (complete mini tablets (Roche) supplemented with 1 mM PMSF) on ice. Nuclei were sedimented by centrifugation (1,000×*g*), resuspended in Buffer C (10 mM Hepes (pH 7.6), 3 mM $MgCl_2$, 100 mM KCl, 0.1 mM EDTA, 10% glycerol, 1 mM DTT, and protease inhibitors), and lysed by the addition of ammonium sulfate to a final concentration of 0.3 M. Soluble nuclear proteins were separated by insoluble chromatin fraction by ultracentrifugation (100,000×*g*) and precipitated with 0.3 mg/ml ammonium sulfate for 20 min on ice. Protein precipitate was isolated by ultracentrifugation (100,000×*g*), and resuspended in HEMG-0 buffer (25mM HEPES (pH 7.9), 0.1mM EDTA, 12.5mM MgCl2, 100mM KCl) for glycerol gradient analyses. 800 ug of protein was overlaid on to a 10ml 10-30% glycerol (in HEMG buffer) gradient prepared in a 14×89 mm polyallomer centrifuge tube (Beckman, part# 331327). Tubes were placed in a SW-40 swing bucket rotor and centrifuged at 4 degrees for 16 hours at 40,000 RPM. 0.5 ml fractions were harvested and used in gel electrophoresis and subsequent western blotting analyses.

Western Blots

Nuclei were isolated from cells with Buffer A (25 mM Hepes, pH 7.6, 5 mM $MgCl_2$, 25 mM KCl, 0.05 mM EDTA, 10% glycerol, 0.1% NP-40) and lysed for 30 min in RIPA buffer (10mM Tris pH 7.4, 150mM NaCl, 0.1% SDS, 0.5% sodium deoxycholate, 1% Triton X-100, 1mM EDTA). Chromatin was either spun out or samples were sonicated prior to BCA analysis. Equal amounts of protein were boiled in gel loading buffer and loaded onto 4-10% BisTris NuPage gels. After transfer, blots were blocked in 5% BSA and incubated with anti-Brg, anti-TopoIIα, anti-pTyr (Millipore clone 4g10 05-321), anti-pSer (Millipore clone 4A4 05-1000), or anti-Ubiquitin (Santa Cruz clone P4D1 sc-8017). Proteins were detected using the LICOR detection system or ECL/autoradiography for SUMO-TopoIIα.

Chromatin Association Assay

Nuclei were isolated using Buffer A and re-suspended in 20 mM Tris-HCl pH 7.6, 3 mM EDTA at 60 mill cells/mL. Samples of 25 μL were alloquotted into tubes and NaCl concentrations were adjusted to a final volume of 50 μL. Samples were gently mixed and incubated on ice for 20 min and centrifuged at high speed for 20 min to isolate chromatin. The lysate was removed and the chromatin pellet was re-suspended in 120 μL gel loading dye. The pellet was solubilized using sonication and the association of TopoIIα to chromatin was analyzed using western blotting.

ATPase Assay

ATPase assay was adapted from the literature[31]. Immunoprecipitations were performed as described above with anti-Brg antibody. IPs were washed a final time with 10 mM TrisHCl pH 7.5, 50 mM NaCl, 5 mM $MgCl_2$, 1 mM DTT and resuspended in 20 μL assay buffer (10 mM Tris-HCl pH 7.5, 50 mM NaCl, 5mM $MgCl_2$, 20% glycerol, 1 mg/ml BSA, 0.5 mM ATP, 20 nM plasmid DNA, 50 μCi/mL γ-^{32}P ATP, 1 mM DTT, protease inhibitors). The reaction was agitated at 37 °C for 1h (or when approximately 50% of ATP was converted to inorganic phosphate). Reaction mixture (0.5 uL) was spotted onto PEI cellulose plates and thin layer chromatography was performed in 0.5M LiCl, 1M formic acid. The plates were dried and imaged using phosphorimaging. The enzymatic activity was quantitated as a ratio of product (^{32}P-P_i) to starting material (γ-^{32}P ATP). Values were normalized to the activity of BrgWT (100%) and vector control (0%) cells

Chromatin Immunoprecipitation

For the Brg1 ChIP, 40 mill ES cells were fixed for 12 minutes in 1% formaldehyde at room temperature. Nuclei were sonicated in 1 mL ChIP Lysis Buffer (50 mM HEPES pH 7.5, 150 mM NaCl, 2 mM EDTA, 1% Triton X-100, 0.1% SDS) to yield fragments between 200-500 bp. 500 μl of lysate was incubated with 5 μg of anti-Brg1 (Crabtree Lab) or 5 μg anti-rabbit IgG and rotated overnight at 4° C and then for 2h with 20 μl Protein A/G Dynabeads. After five washes with ChIP Lysis Buffer and one wash in TE, DNA was eluted by boiling in 10% Chelex slurry.

The etoposide ChIP of TopoIIα was adapted from the literature[26]. Specifically, 20 million ES cells were treated with 100 μM etoposide for 10 minutes. Cells were washed once with PBS and lysed with 1 ml of a buffer containing 1% Sarkosyl, 10 mM Tris-HCl (pH 7.5), 10 mM EDTA, and protease inhibitor. A solution of 7 M CsCl (7 M) was added to a final concentration of 0.5 M and the lysate was sonicated to yield fragments between 200-500 bp. ChIP buffer (300 μL) was added to 300 μl of lysate for a final concentration of 50 mM HEPES pH 7.5, 300 mM NaCl, 1 mM EDTA, 1 % Triton X-100, 0.1 % DOC, and 0.1% SDS and 3 μg Anti-TopoIIα (sc-365916) prebound to 20 μl Protein G Dynabeads was added. The lysate was rotated overnight at 4° C and washed four times with ChIP lysis buffer, one time with LiCl buffer (10 mM Tris pH 8.0, 0.25 M LiCl, 0.5 % NP-40, 0.5% DOC, 1 mM EDTA) and one time with TE. The DNA was eluted with 300 μl of 1% SDS, 0.1 M $NaHCO_3$ for 20 minutes and removed from the beads. The solution was adjusted to 200mM NaCl, 10mM EDTA, 40mM Tris pH 6.5 and 0.2 mg/mL RNase A was added for 30 min at 37° C. Proteinase K was added to 0.03 mg/ml and digested overnight at 55° C. The DNA

was extracted with phenol/chloroform and precipitated with ethanol for analysis by qPCR. Primers used for ChIP-qPCR are available upon request.

ChIP-seq and Analysis

The library preparation and sequencing was performed as previously described[32]. Raw ChIP-seq reads were mapped to the *Mus musculus* genome (build mm9/NCBI37) using the short-read aligner Bowtie (version 0.12.7)[33]. Peaks were then called using Model-base Analysis of ChIP-seq (MACS) (version 1.4.1)[34]. Further analysis was aided by the Bedtools suite (version 2.16.2) [35]. Genome annotations were acquired from the UCSC Genome Browser (http://genome.ucsc.edu/)[36,37]. We also uploaded our data to the genome browser, which was used to produce screenshots of chromatin binding/modification profiles at individual loci.

Topoisomerase Activity Assay

Reactions contain: 150 ng kinetoplast DNA (Topogen), 50 mM Tris-HCl, pH 8.0, 150 mM NaCl, 10 mM $MgCl_2$, 2 mM ATP, a standard TopoIIα IP or varying amounts of recombinant TopoIIα (Topogen).

Lentiviral Infection

293XTs were transfected with lentiviruses containing vector alone, wild-type Brg1, Brg1 point mutants, wild-type hTopoIIα, or hTopoIIαS1524A or with vectors containing hairpins to *brg*, (TRCN0000071386), *arid1a* (TRCN0000071395, Origene TG517733), or *top2a* (V2LMM_11295). 48 hours later, supernatants were collected and centrifuged at 20,000 rpm for 2 hours. Viral pellets were resuspended in PBS and used to infect ES cells in suspension or MEFs by spinfection. Cells were selected with puromycin and collected 48-96 hours postinfection for analysis.

Supplementary Material

Refer to Web version on PubMed Central for supplementary material.

Acknowledgments

We would like to acknowledge the DNA Sequencing Core facility of NHLBI for sequencing the ChIP-Seq libraries. This work was supported by the NIH (G.R.C.), The American Cancer Society (E.C.D.), The Helen Hay Whitney Foundation (D.C.H), and the Division of Intramural Research program of NHLBI (K.Z). G.R.C. is an investigator in the Howard Hughes Medical Institute.

References

1. Kadoch C, et al. Proteomic and Bioinformatic Analysis of mSWI/SNF (BAF) Complexes Reveals Extensive Roles in Human Malignancy. Nature Genetics. 2013 In preparation.
2. You JS, Jones PA. Cancer Genetics and Epigenetics: Two Sides of the Same Coin? Cancer Cell. 2012; 22:9–20. [PubMed: 22789535]
3. Clapier CR, Cairns BR. The biology of chromatin remodeling complexes. Annu Rev Biochem. 2009; 78:273–304. [PubMed: 19355820]
4. Ho L, et al. esBAF facilitates pluripotency by conditioning the genome for LIF/STAT3 signalling and by regulating polycomb function. Nat Cell Biol. 2011; 13:903–913. [PubMed: 21785422]

5. Wilson BG, et al. Epigenetic antagonism between polycomb and SWI/SNF complexes during oncogenic transformation. Cancer Cell. 2010; 18:316–328. [PubMed: 20951942]
6. Parsons DW, et al. The genetic landscape of the childhood cancer medulloblastoma. Science. 2011; 331:435–439. [PubMed: 21163964]
7. Pugh TJ, Cho YJ, et al. Medulloblastoma exome sequencing uncovers subtype-specific somatic mutations within a broad landscape of genetic heterogeneity. Nature. 2012
8. Jones DTW, et al. Dissecting the genomic complexity underlying medulloblastoma. Nature. 2012; 488:100–105. [PubMed: 22832583]
9. Robinson G, et al. Novel mutations target distinct subgroups of medulloblastoma. Nature. 2012; 488:43–48. [PubMed: 22722829]
10. Love C, et al. The genetic landscape of mutations in Burkitt lymphoma. Nature Genetics. 2012; 44:1321–1325. [PubMed: 23143597]
11. Richter J, et al. Recurrent mutation of the ID3 gene in Burkitt lymphoma identified by integrated genome, exome and transcriptome sequencing. Nature Genetics. 2012; 44:1316–1320. [PubMed: 23143595]
12. Carpenter AJ, Porter AC. Construction, characterization, and complementation of a conditional-lethal DNA topoisomerase IIalpha mutant human cell line. Mol Biol Cell. 2004; 15:5700–5711. [PubMed: 15456904]
13. Lou Z, Minter-Dykhouse K, Chen J. BRCA1 participates in DNA decatenation. Nat Struct Mol Biol. 2005; 12:589–593. [PubMed: 15965487]
14. Dawlaty MM, et al. Resolution of sister centromeres requires RanBP2-mediated SUMOylation of topoisomerase IIalpha. Cell. 2008; 133:103–115. [PubMed: 18394993]
15. Ramamoorthy M, et al. RECQL5 cooperates with Topoisomerase II alpha in DNA decatenation and cell cycle progression. Nucleic Acids Res. 2012; 40:1621–1635. [PubMed: 22013166]
16. Ho L, et al. An embryonic stem cell chromatin remodeling complex, esBAF, is essential for embryonic stem cell self-renewal and pluripotency. Proc Natl Acad Sci U S A. 2009; 106:5181–5186. [PubMed: 19279220]
17. Johnson M, Phua HH, Bennett SC, Spence JM, Farr CJ. Studying vertebrate topoisomerase 2 function using a conditional knockdown system in DT40 cells. Nucleic Acids Res. 2009; 37:e98. [PubMed: 19494182]
18. Downes CS, et al. A topoisomerase II-dependent G2 cycle checkpoint in mammalian cells. Nature. 1994; 372:467–470. [PubMed: 7984241]
19. Luo K, Yuan J, Chen J, Lou Z. Topoisomerase IIalpha controls the decatenation checkpoint. Nat Cell Biol. 2009; 11:204–210. [PubMed: 19098900]
20. Sakaguchi A, Kikuchi A. Functional compatibility between isoform alpha and beta of type II DNA topoisomerase. J Cell Sci. 2004; 117:1047–1054. [PubMed: 14996935]
21. Khavari PA, Peterson CL, Tamkun JW, Mendel DB, Crabtree GR. BRG1 Contains a Conserved Domain of the SWI2/SNF2 family necessary for normal mitotic growth and transcription. Nature. 1993; 366:170–174. [PubMed: 8232556]
22. Kool M, et al. Molecular subgroups of medulloblastoma: an international meta-analysis of transcriptome, genetic aberrations, and clinical data of WNT, SHH, Group 3, and Group 4 medulloblastomas. Acta Neuropathol. 2012; 123:473–484. [PubMed: 22358457]
23. Northcott PA, et al. Medulloblastomics: the end of the beginning. Nature Reviews Cancer. 2012; 12:818–834. [PubMed: 23175120]
24. Ho L, et al. An embryonic stem cell chromatin remodeling complex, esBAF, is an essential component of the core pluripotency transcriptional network. Proc Natl Acad Sci U S A. 2009; 106:5187–5191. [PubMed: 19279218]
25. Stros M, Bacikova A, Polanska E, Stokrova J, Strauss F. HMGB1 interacts with human topoisomerase IIalpha and stimulates its catalytic activity. Nucleic Acids Res. 2007; 35:5001–5013. [PubMed: 17636313]
26. Sano K, Miyaji-Yamaguchi M, Tsutsui KM, Tsutsui K. Topoisomerase II beta Activates a Subset of Neuronal Genes that Are Repressed in AT-Rich Genomic Environment. Plos One. 2008; 3

27. Capranico G, Jaxel C, Roberge M, Kohn KW, Pommier Y. Nucleosome positioning as a critical determinant for the DNA cleavage sites of mammalian DNA topoisomerase II in reconstituted simian virus 40 chromatin. Nucleic Acids Res. 1990; 18:4553–4559. [PubMed: 2167470]
28. Sperling AS, Jeong KS, Kitada T, Grunstein M. Topoisomerase II binds nucleosome-free DNA and acts redundantly with topoisomerase I to enhance recruitment of RNA Pol II in budding yeast. Proc Natl Acad Sci U S A. 2011; 108:12693–12698. [PubMed: 21771901]
29. Bourgo RJ, et al. SWI/SNF deficiency results in aberrant chromatin organization, mitotic failure, and diminished proliferative capacity. Mol Biol Cell. 2009; 20:3192–3199. [PubMed: 19458193]
30. Janssen A, van der Burg M, Szuhai K, Kops GJ, Medema RH. Chromosome segregation errors as a cause of DNA damage and structural chromosome aberrations. Science. 2011; 333:1895–1898. [PubMed: 21960636]
31. Bultman SJ, Gebuhr TC, Magnuson T. A Brg1 mutation that uncouples ATPase activity from chromatin remodeling reveals an essential role for SWI/SNF-related complexes in beta-globin expression and erythroid development. Genes Dev. 2005; 19:2849–2861. [PubMed: 16287714]
32. Barski A, et al. High-resolution profiling of histone methylations in the human genome. Cell. 2007; 129:823–837. [PubMed: 17512414]
33. Langmead B, Trapnell C, Pop M, Salzberg SL. Ultrafast and memory-efficient alignment of short DNA sequences to the human genome. Genome Biol. 2009; 10:R25. [PubMed: 19261174]
34. Zhang Y, et al. Model-based analysis of ChIP-Seq (MACS). Genome Biol. 2008; 9:R137. [PubMed: 18798982]
35. Quinlan AR, Hall IM. BEDTools: a flexible suite of utilities for comparing genomic features. Bioinformatics. 2010; 26:841–842. [PubMed: 20110278]
36. Kent WJ, et al. The human genome browser at UCSC. Genome Res. 2002; 12:996–1006. [PubMed: 12045153]
37. Meyer LR, et al. The UCSC Genome Browser database: extensions and updates 2013. Nucleic Acids Res. 2012

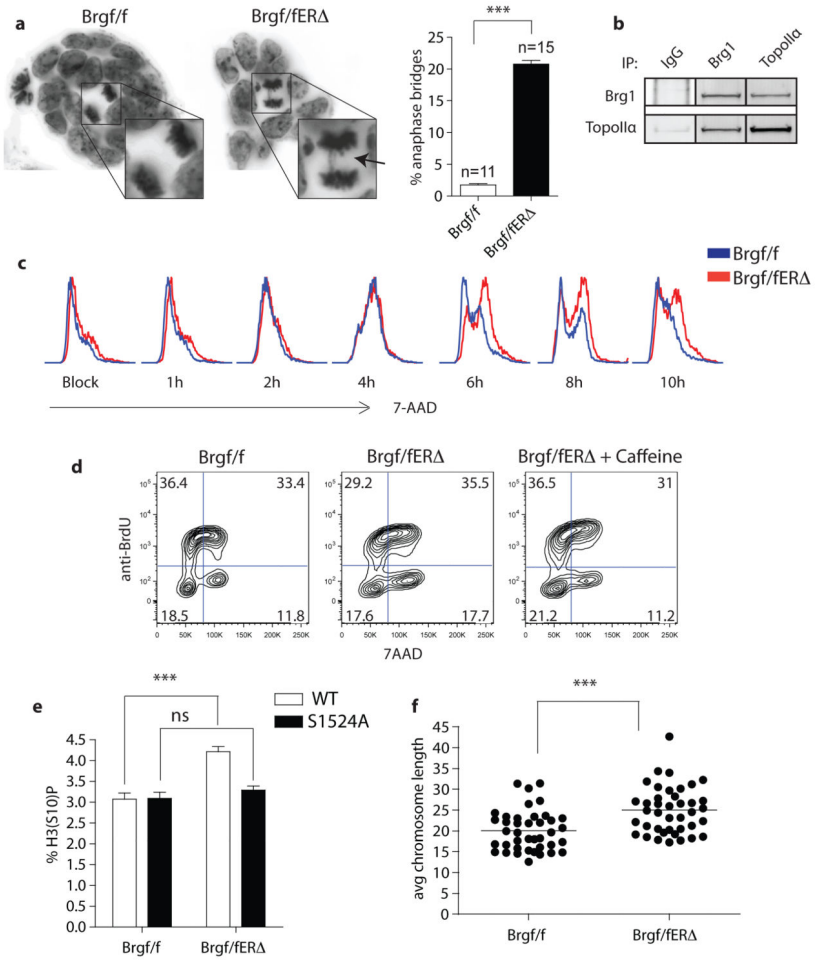

Figure 1. Brg1 associates with Topoisomerase IIα and regulates its function

a, Anaphase bridges in Brgf/f and Brgf/fERΔ ES cells. Data represent n number of slides from four independent experiments +/− SEM. **b**, Co-IP of Brg1 and TopoIIα from nuclear lysates. **c,** DNA content in Brgf/f and Brgf/fERΔ ES cells after release from double thymidine block. **d**, Cell cycle analysis of Brgf/f and Brgf/fERΔ ES cells with or without caffeine, an ATM/ATR inhibitor. **e,** Data represent 5 independent H3(S10)P cell cycle analyses +/− SEM. **f,** Data represent the mean of the average chromosome length per cell from 40 cells from metaphase spreads of Brgf/f and Brgf/fERΔ MEFs from 2 independent experiments.

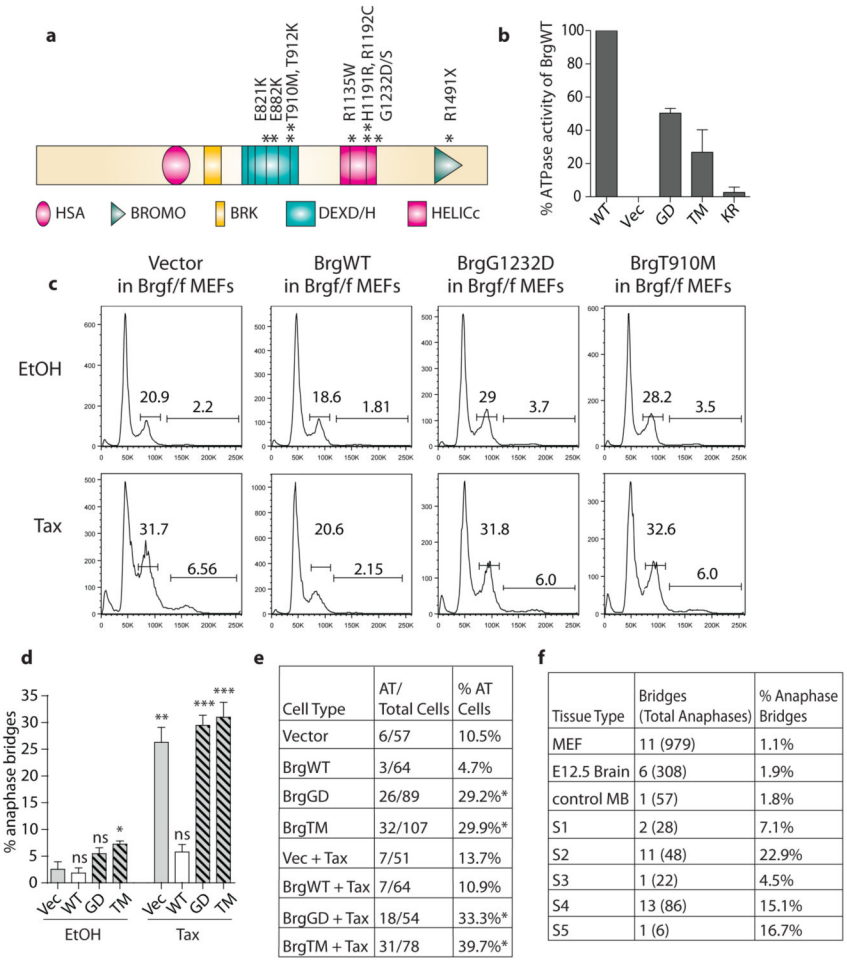

e

Cell Type	AT/ Total Cells	% AT Cells
Vector	6/57	10.5%
BrgWT	3/64	4.7%
BrgGD	26/89	29.2%*
BrgTM	32/107	29.9%*
Vec + Tax	7/51	13.7%
BrgWT + Tax	7/64	10.9%
BrgGD + Tax	18/54	33.3%*
BrgTM + Tax	31/78	39.7%*

f

Tissue Type	Bridges (Total Anaphases)	% Anaphase Bridges
MEF	11 (979)	1.1%
E12.5 Brain	6 (308)	1.9%
control MB	1 (57)	1.8%
S1	2 (28)	7.1%
S2	11 (48)	22.9%
S3	1 (22)	4.5%
S4	13 (86)	15.1%
S5	1 (6)	16.7%

Figure 2. Expression of Medulloblastoma-associated Brg1 mutants phenocopies Topoisomerase IIα inhibition

a, Somatic mutations in BRG1 found in medulloblastoma. **b,** The DNA-stimulated ATPase activity of BAF complexes from BrgWT, BrgGD, BrgKR, BrgTM, and vector control-expressing Brgf/fERΔ cells +/− SEM. **c**, Cell cycle analysis of Brgf/f MEFs expressing BrgWT, BrgGD, BrgTM, or vector, treated with ethanol or tamoxifen (Tax). **d**, Cells were prepared as in **(c)** and the mean frequency of anaphase bridges +/− SEM from three independent experiments was measured. **e**, Cells were prepared as in **(c)** and harvested for metaphase spreads. The number of cells with greater than 40 chromosomes (AT) was quantitated from >50 cells. Significance was calculated relative to vector control, ethanol-treated Brgf/f cells where *p<0.05, **p<0.01, ***p<0.0001. **f**, Various tissues were sectioned and scored for the number of anaphase bridges of total anaphases.

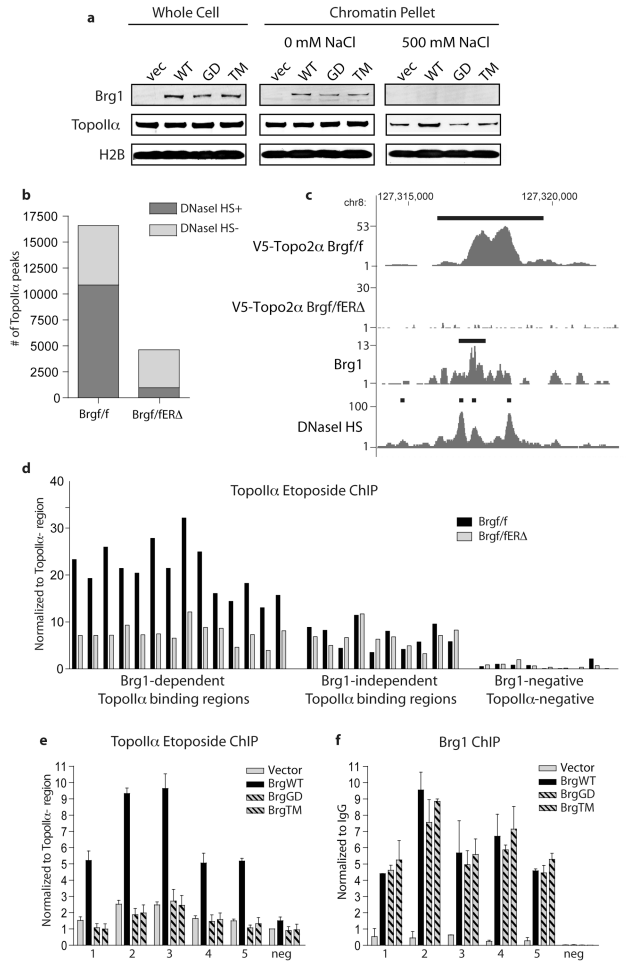

Figure 3. Brg1 facilitates the binding of Topoisomerase IIα to chromatin *in vivo* through ATPase-dependent chromatin remodeling activity

a, Chromatin pellets isolated from nuclei of BrgWT, BrgGD, BrgTM, and vector-expressing Brgf/fERΔ ES cells lysed in +/− 500mM NaCl. **b**, The number of DNase I hypersensitive TopoIIα peaks of the total number of TopoIIα peaks from TopoIIα ChIP-seqs in Brgf/f and Brgf/fERΔ ES cells. **c**, Representative ChIP-seq tracks for TopoIIα (in Brgf/f and Brgf/fERΔ ES cells), Brg1, and DNase I hypersensitivity. **d**, TopoIIα ChIP-qPCR confirmation from Brgf/f and Brgf/fERΔ ES cells. **e**, TopoIIα ChIP-qPCR confirmation from BrgWT, BrgGD, BrgTM, and vector control-expressing Brgf/fERΔ ES cells. **f**, Brg1 ChIP-qPCRs from BrgWT, BrgGD, BrgTM, and vector control-expressing Brgf/fERΔ ES cells. **e, f,** Data represent means of triplicate experiments +/− SEM.

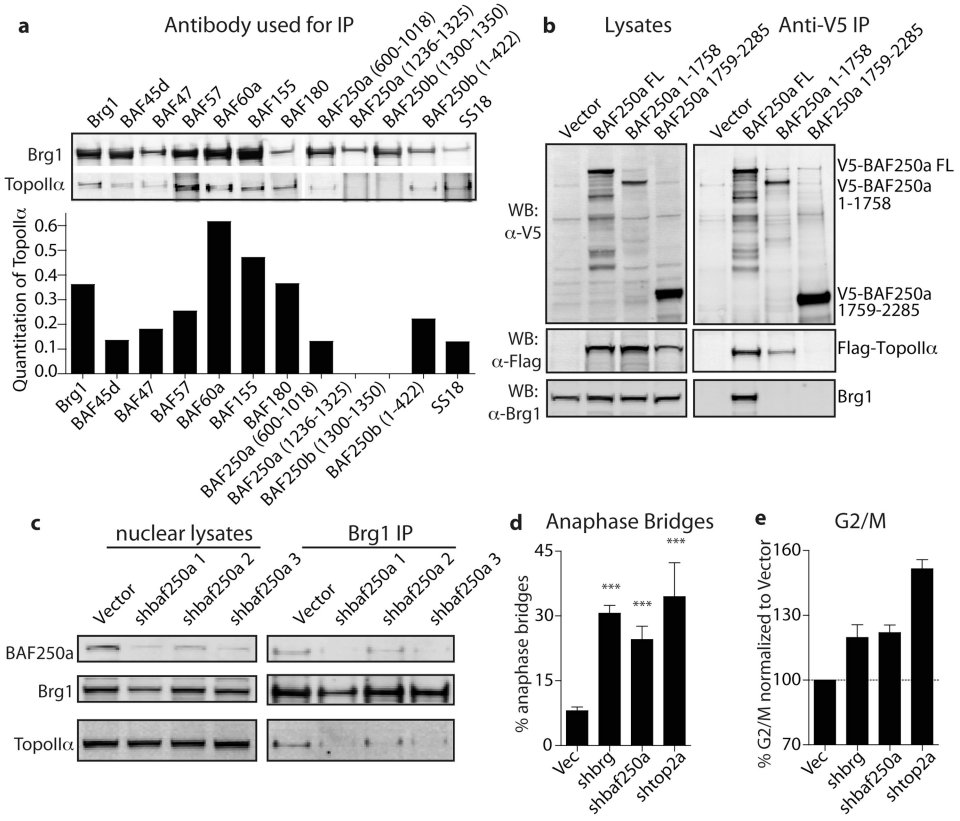

Figure 4. Topoisomerase IIα associates with the BAF complex through BAF250a

a, IPs from ES nuclear lysates. Quantitation of the precipitated TopoIIα is shown. **b**, V5 was precipitated from 293Ts that had been transfected with Flag-TopoIIα and either vector, V5-tagged full-length BAF250a (BAF250a FL), or V5-tagged BAF250a fragments. Lysates and anti-V5 precipitates were blotted for anti-V5, anti-Flag, and anti-Brg1. **c**, Brg1 was IP'ed from ES cells following BAF250a knockdown. **d,** MEFs with knockdown of Brg1, BAF250a or TopoIIα. Anaphase bridge frequency is calculated for seven experiments +/− SEM. Significance was calculated relative to vector control cells where *p<0.05, **p<0.01, ***p<0.0001. **e**, Cell cycle analysis of MEFs from **(d).** Data represent the mean of the % of G_2/M cells normalized to vector control from four experiments +/− SEM.